International Journal of Technology

http://ijtech.eng.ui.ac.id

Research Article

Carboxylation Reaction of Epichlorohydrin: Spectra-Based Experimental and Analytical System for Online Reaction Study

Maria Atlaskina [1,*], Zakhar Markin [2], Kirill Smorodin [1], Sergey Kryuchkov [1], Pavel Tiuleanu [1], Alexander Sysoev [1], Anton Petukhov [2], Artem Atlaskin [1], Olga Kazarina [1], Andrey Vorotyntsev [2], Ilya Vorotyntsev [1]

[1]*Laboratory of SMART Polymeric Materials and Technologies, Mendeleev University of Chemical Technology of Russia, Miusskaya square, 9, Moscow, 125047 Russia*
[2]*Chemical Engineering Laboratory, Lobachevsky State University of Nizhny Novgorod, 23 Gagarin Avenue, Nizhny Novgorod, 603022, Russia*
[*]*Corresponding author: atlaskina.m.e@gmail.com; Tel.: +74999788660*

Abstract: A significant challenge of Carbon Capture and Storage strategy is the need to store or convert carbon dioxide (CO_2) into valuable products. Among the various catalysts for CO_2 conversion to cyclic carbonate, ionic liquid (IL) has shown superior performance due to the environmental friendliness and high selectivity. This shows the need for analysis to understand the mechanism of CO_2 conversion. Therefore, this study aimed to conduct an experimental and analytical setup for in-situ/operando studies of carboxylation reaction of unsaturated compound oxides (epichlorohydrin) at atmospheric or elevated pressure in a closed volume FTIR (Fourier Transform Infrared) and Raman multispectroscopy base with immersion probes and mass spectra endpoint. IL 1-(2-hydroxyethyl)-3-methylimidazolium bromide ([C_2OHmim][Br]) was used as catalyst for the reaction. The results showed that Raman spectra were not a suitable method of analysis for the selected system due to the presence of strong luminescence. By using IR spectroscopy, the coordination of substrate onto catalyst was shown to occur because of hydrogen bonds between the imidazole proton at C^2 position of imidazole ring and the hydroxyl group of the substituent in IL. Based on the obtained data, the mechanism of catalytic reaction was proposed.

Keywords: Catalysis; CO_2 conversion; Cyclic carbonate; Ionic liquid; IR spectra

1. Introduction

Carbon dioxide (CO_2) emission is a symbol of modern environmental challenges in the context of global warming and natural disasters caused by human activity. The issue is further increased by progressive economic growth and a significant rise in energy consumption due to the rapid development of industry (Whang et al., 2019). As the dominant product of the exothermic reaction of carbon-containing fuel combustion, the amount of CO_2 produced reaches 30 billion tons per year (Le Quéré et al., 2016) serving as the largest non-recyclable waste. Despite the rapid development in the use of alternative energy sources, significantly limiting the application of carbon-containing substances in the energy industry is challenging. One of the most effective solutions to reduce CO_2 emission is the concept of gas capture and subsequent processing into valuable products or line use.

This work was supported by the 'Russian Science Foundation' funded by 'project No. 22-79-10302

https://doi.org/10.14716/ijtech.v16i4.7596
Received January 2025; Revised February 2025; Accepted April 2025

The classical method of CO_2 capture is chemical absorption with organic solvents or membranes (Kryuchkov et al., 2024; Kartohardjono et al., 2017). Among various CO_2 absorbents, monoethanolamine is the best-known, which reacts with CO_2 to form carbamate, a process called amine scrubbing. The sorption capacity of an aqueous solution of monoethanolamine reaches 1 mol CO_2·mol amine^{-1} (Kazarina et al., 2022; Shariff et al., 2016; Kadiwala et al., 2010; Jou et al., 1995). However, the high energy intensity of the process due to absorbent regeneration step and high capital costs are significant disadvantages requiring the search for alternative methods.

Adsorption methods of CO_2 capture are less preferable because the capacity often does not exceed 5-7 mmol·g^{-1}. The most common adsorbers are solids such as activated carbons (Cruz et al., 2023; Yuan et al., 2023), metal-organic framework (Asgharnejad et al., 2018; Arstad et al., 2008), graphite composites (Kusrini et al., 2018), and zeolitic imidazolate framework (Souza-Filho et al., 2024; Mohammadi and Nakhaei Pour, 2023). Other disadvantages include low kinetic characteristics, insufficient mechanical strength of some materials, and minimal selectivity.

In recent years, the idea of producing formic acid (Liu et al., 2019; Lu et al., 2014), ethylene (Schreiber, 2024; Ozden et al., 2021; Li et al., 2019; Dinh et al., 2018), methane (Su et al., 2024; Zhang et al., 2021; 2020) by electrochemical reduction of CO_2 has become very popular. The advantages of this method of recovery include the ease of reaction control through electrode temperature and potential, as well as modularity and compactness of the system. However, there are numerous disadvantages such as low energy efficiency, slow recovery kinetics, and high overvoltage (Yaashikaa et al., 2019; Kumar et al., 2016; Sridhar et al., 2009).

One of the most promising routes to reduce CO_2 emission is recycling (conversion) into cyclic carbonate or other valuable products (Anggerta et al., 2025; Madani et al., 2024). This process is attractive due to the possibility of obtaining useful chemicals including environmental friendliness and high energy efficiency. Generally, cyclocarbonate is used as solvents (Ayuso et al., 2023; Jessop, 2011), battery components (Jin et al., 2024; Qian et al., 2022; Tillmann et al., 2014), and construction purposes (Liu et al., 2015). The synthesis of cyclic carbonate by cycloaddition of CO_2 to epoxides is more promising in comparison with traditional method using phosgene because of toxicity and by-products (Kamphuis et al., 2019). Despite widespread application as substrate, propylene or ethylene oxides are obtained from non-renewable raw materials, which reduces attractiveness in the framework of green chemistry. An attractive substrate is (chloromethyl) oxirane (epichlorohydrin (ECH)), which can be obtained from a renewable feedstock glycerol. Furthermore, the conversion of ECH to cyclic carbonate is easier than other epoxides due to the high electronegativity of the chlorine atom. To further enhance the process, ionic liquid (IL) catalyst [Heemim][$ZrCl_5$] has been tested for the synthesis of cyclic carbonate from various epoxides (Hu et al., 2015). The results show that cyclic carbonate with high yield in the shortest time (97% in 2 hours) is obtained using epichlorohydrin.

The process of CO_2 conversion in this study takes place in the presence of catalysts. Various catalysts have been explored for this purpose, including zeolite imidazolate frameworks (ZIF) (Olaniyan and Saha, 2020), aluminum complexes (North, 2012), metal-organic frameworks (MOF) (Zhang and Xu, 2024; Shah et al., 2022; Yulia et al., 2019; Maina et al., 2017), and organocatalysts such as triethanolamine (Yan et al., 2023). Among these catalysts, IL has shown superior performance due to the low volatility, environmental friendliness, ability to markedly improve the efficiency and selectivity of the chemical reaction, and diversity of structures (Hu et al., 2015; Wang et al., 2014; Sun et al., 2008). Currently, several studies have focused on density functional theory (DFT) description of the reaction mechanism, which gives only approximate results (Zha et al., 2020; Liu et al., 2015; Whiteoak et al., 2014). This shows the need for validation by experiment to ensure a more accurate understanding of the process.

In this study, the reaction mechanism for carboxylation of unsaturated compound oxides, epichlorohydrin, in the presence of catalyst 1-(2-hydroxyethyl)-3-methylimidazolium bromide was presented and proved. To achieve the objective, an experimental and analytical complex for in-situ/operando studies was developed based on FTIR and Raman multispectroscopy with

immersion probes. The complex was designed to explore carboxylation reaction of unsaturated compounds at atmospheric or elevated pressure in a closed volume. On the basis of in-situ/operando FTIR and Raman spectra data, the mechanism of the investigated reaction was proposed. The coordination of the substrate to catalysts was shown to occur because of hydrogen bonds between the imidazole proton in C^2 position of the imidazole ring and the hydroxyl group of the substituent in IL.

2. Method

2.1. Chemicals and Materials

Chemicals used to synthesize catalysts were 2-bromoethanol (99 wt.%, originated from Sigma-Aldrich (Schnelldorf, Germany)), 1-methylimidazole (99 wt.%, originated from Acros Organics (Geel, Belgium)), ethyl acetate (< 99 wt.%, originated from Aldosa, Moscow, Russia) and phosphoric anhydride (98 wt.%, originated from CJSC Khimreaktiv (Nizhny Novgorod, Russia)). Furthermore, Epichlorohydrin (>99 wt.%) obtained from Chemical Line (Saint Petersburg, Russia) and CO_2 (≥99.99 vol.%) purchased from Monitoring LLC (Saint Petersburg, Russia) were used to explore carboxylation reaction of unsaturated compound oxides.

2.2. Catalyst synthesis

To synthesize IL 1-(2-hydroxyethyl)-3-methylimidazolium bromide ([C_2OHmim][Br]), an equimolar amount of 2-bromoethanol was added to 1-methylimidazole and heated to 70 degrees with stirring in an inert gas atmosphere. Subsequently, the synthesized IL was washed several times with ethyl acetate and dried over phosphoric anhydride (Atlaskina et al., 2025).

2.3. Analytical complex

As part of this study, an experimental and analytical complex for in-situ/operando studies was developed based on FTIR and Raman multispectroscopy with submersible probes, as shown in Figure 1. The complex was intended for the study of carboxylation reaction of unsaturated compounds at atmospheric or elevated pressure in a confined volume. The experimental setup had mass spectra end, which allowed monitoring of the changes in the concentration of initial components (CO_2 and epichlorohydrin) during the experiment.

The experimental setup designed for carboxylation reaction of unsaturated oxides at elevated pressure in a confined space is shown in Figure 1. The apparatus consists of a reactor (1) made of stainless steel 08X16H11M3 with one technological opening for gas inlet and outlet. The reactor also contains catalyst [C_2OHmim][Br] and a starting substance, namely epichlorohydrin, alongside the necessary control and measuring equipment. A three-port, two-position SS-83XTS4 valve (2) (Swagelok, USA) is used to switch between the reactor operation modes (gas inlet, gas analysis). In this system, at the start of the experiment, CO_2 gas is introduced into the internal volume of the reactor. After a certain period of time, the three-port valve is switched to the position connecting the reactor with mass spectra complex to analyze the composition of the gas medium. Additionally, the reactor is equipped with probes to monitor the reaction process. The control is performed spectrometrically with the help of a multispectral complex through IR and Raman probes immersed in the reaction mixture (liquid phase).

In this system, CO_2 gas is supplied from a cylinder (3) through a pressure regulator 072S-0050C-1S-5 (Drastar LTD, Korea) and a gas flow regulator (4) El-Flow Prestige FG-201CV (Bronkhorst, the Netherlands). At the reactor outlet, there is a gas pressure regulator (5) functioning in the mode of maintaining constant pressure 'up to itself', El-Press P-702CM (Bronkhorst, the Netherlands). The outlet from the reactor is connected to mass spectra complex (6) consisting of membrane and turbomolecular vacuum pumps (Pfeiffer Hi-Cube ECO 300), which provide the primary discharge in the zone of sample input. The pressure in this cavity is determined using a pressure transmitter (7) (Pfeiffer MPT200). Furthermore, the vacuum post is connected to mass spectra chamber (8) (Pfeiffer PrismaPro QMG 250 M2), where the vacuum is provided by a second vacuum post (9)

(Pfeiffer Hi-Cube 80 Eco) and the level is determined by a second pressure transducer of the same model. The reactor is located on a C-Mag HS 7 control magnetic stirrer (10) (IKA-Werke, Germany) for constant stirring of the reaction mixture. Mass spectra are obtained through PrismaPro QMG 250 M2 1 – 200 u under selected ion monitoring (SIM) mode at 2000 uA emission current, 70 eV electron energy, and 9000 meV ion energy.

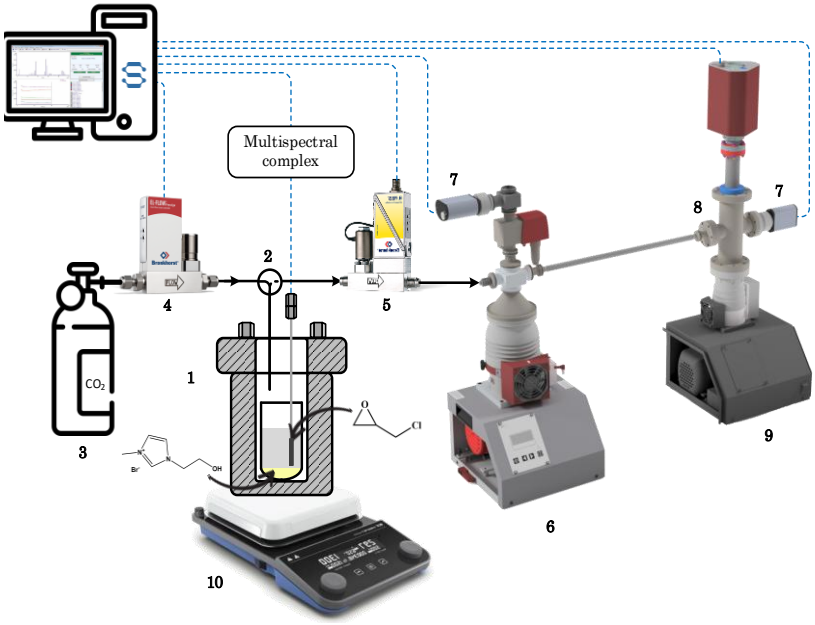

Figure 1 Schematic diagram of the experimental setup for studying concentration profiles of the reaction occurring at elevated pressure in the atmosphere of CO_2 in a confined volume

3. Results and Discussion

3.1. Mass spectra

Before the experiment, based on the spectrum presented in NIST library, the mass-to-charge ratio m/z = 57 was selected to track the concentration of epichlorohydrin (NIST U.S. Department of Commerce, 2014). To investigate the concentration profiles of epichlorohydrin carboxylation reaction, a minimum of 5 cycles were performed. These included reactor preparation (washing from the initial reaction components, vacuumisation of the system, CO_2 inlet, and selection of the gas medium (in case of the process in a confined volume). Changes in the concentration of epichlorohydrin and CO_2 during the reaction of carboxylation of unsaturated compounds oxides are presented in Figure S1 (Supplementary File). The concentration profiles of CO_2 and epichlorohydrin during carboxylation reaction of epichlorohydrin led to the concentration dependencies of these components on the duration of the experiment. The dependences were obtained from mass spectra obtained for characteristic mass-to-charge ratios of CO_2 and epichlorohydrin (m/z = 44 and m/z = 57). In this study, 7 experiments were performed and the values of CO_2 and epichlorohydrin concentrations were averaged, as shown in Figure S1. Observation from dependences showed that in the experiment, the concentration of epichlorohydrin decreased, reaching a minimum constant value in approximately 550 min. Similarly, the concentration of CO_2 in the flow of binary gas mixture increased in the experiment. It was also observed that epichlorohydrin contained in the reactor was consumed during carboxylation reaction, indirectly indicating the successful experiment.

Figure S2 (Supplementary File) shows the results of CO_2 and epichlorohydrin concentration profiles during carboxylation reaction of epichlorohydrin. As part of the experiment in Figure 1, the gaseous medium was sampled at the end of the reaction. The stream formed by the binary mixture was fed into mass spectra system to analyze the composition of the gas mixture. The experiment

including preparation (washing) of the reactor, loading of initial components (IL, epichlorohydrin), and removal of atmospheric air and CO_2 inlet was repeated 5 times. After the experiment, mass spectra of the binary gas system were obtained and averaged. The results were presented as dependent on the concentration of mixture components (O_2 and epichlorohydrin) regarding the duration of the experiment.

From the presented dependences in Figure S2, the concentration profiles show that at the initial stage of gas withdrawal from the reactor, the gas mixture contains residual unreacted epichlorohydrin. However, as the gas medium is withdrawn from the reactor, it is replaced by CO_2, and the concentration of epichlorohydrin sharply decreases in the interval of 75 - 150 min after the start of the experiment. Since the reactions are carried out in excess of CO_2, the concentration of epichlorohydrin in the gas phase gradually decreases and reaches the minimum near zero values at the level of residual impurity.

3.1.1. Spectral data collection

For the convenience of the operation on the multispectrometer, spectral characteristics of all participants of the reaction were obtained for quick identification during the reaction.

3.1.1.1. FTIR

IR spectra of the start of epichlorohydrin and the main product (chloropropylene carbonate) are shown in Figures S3 and S4 (Supplementary File), respectively. Meanwhile, Figure S2 shows IR spectra of catalyst (1-(2-hydroxyethyl)-3-methylimidazolium bromide). Furthermore, IR spectra of epichlorohydrin show characteristic vibrations, but the intensity is not high. For example, the valence vibrations of ether C-O-C (several non-equivalent bonds) appear at 1135 and 1089 cm^{-1}. The intensity of these bonds is low due to the strain and rigidity of the three-membered cycle of epichlorohydrin and the limited amplitude of vibrations. In comparison, the high-intensity band at 758 cm^{-1} corresponds to the valence vibrations of the C-Cl bond. The bands of skeletal deformation vibrations of C-C bonds are shown in the range of less than 1000 cm^{-1}. The valence vibrations of C-H bonds appear at 3060-2920 cm^{-1} and the deformation is observed at 1500-1250 cm^{-1}.

In line with the results, IR spectra of chloropropylene carbonate show characteristic vibrations intensely. A high-intensity band is observed at 1778 cm^{-1}, corresponding to the valence asymmetric vibrations of C=O bond in carbonyl group of carbonate fragment. The valence vibrations of C-O-C ether bonds (several non-equivalent bonds) occur at 1158, 1062, and 1037 cm^{-1}. Additionally, the valence vibrations of C-Cl and C-H bonds are observed at 763 cm^{-1} and 2920-3020 cm^{-1}, with the deformation of C-H bonds occurring at 1500-1250 cm^{-1}.

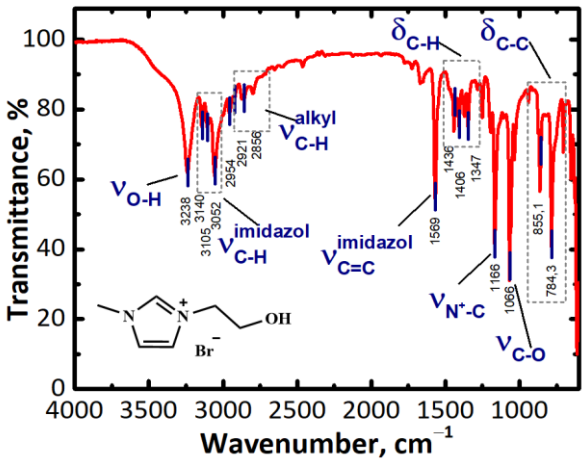

Figure 2 IR spectra of 1-(2-hydroxyethyl)-3-methylimidazolium bromide

IR spectra of 1-(2-hydroxyethyl)-3-methylimidazolium bromide (Figure 3) show intensely characteristic vibrations. A high-intensity band corresponding to the valence vibrations of O-H

bond of hydroxyl group of the substituent is observed at 3238 cm^{-1}. The double C=C bond of the imidazole ring occurs at 1569 cm^{-1}, N^+-C vibrations of the imidazole ring at 1166 cm^{-1}, and C-O bond of hydroxyl group at 1066 cm^{-1}. In addition to these vibrations, IR spectra clearly show C-H valence vibrations in the region of 3000-2800 cm^{-1} for alkyl substituents and 3200-300 cm^{-1} for C-H bonds of the imidazole ring. Deformation vibrations of C-H bonds are also detected in the fingerprint region of1500-1250 cm^{-1}, and C-C skeletal in the range of less than 1000 cm^{-1} (Zaoui et al., 2021; Chaker et al., 2016).

3.1.1.2. Raman

Raman spectra of the initial epichlorohydrin (Figure S5) show bands of C-C deformation vibrations of alkyl chain in the range of 200-400 cm^{-1} with the most pronounced peaks at 231 and 378 cm^{-1}. The characteristic peaks are C-Cl bond vibrations, comprising high intensity at 702 and 728 cm^{-1}, as well as C-O-C bond vibrations at 849 and 933 cm^{-1}. In the fingerprint region, the valence vibrations of C-C bonds of carbon skeleton are clearly visible, appearing as medium and low intensity in the range of 600-1200 cm^{-1}. Peaks of deformation vibrations of CH_2 bonds are observed in the range of 1400-1500 cm^{-1}. Meanwhile, the valence vibrations of carbon-hydrogen bonds of CH_2 groups appear as weak intensity at 2982 cm^{-1}.

As presented in Figure S6, Raman spectra of chloropropylene carbonate (Figure S6) show bands of deformation vibrations of C-C alkyl chain in the range of 200-400 cm^{-1} with the most pronounced peaks at 228 and 339 cm^{-1}. The valence vibrations of C-H bonds of CH_2-groups are also detected at a weak intensity of 2976 cm^{-1}. Furthermore, C-Cl vibrations show high-intensity peaks at 667 and 721 cm^{-1}, as well as C-O-C at 869 and 937 cm^{-1}. The peak of symmetric C=O vibrations of carbonyl group of carbonate fragment is clearly visible. Compared to IR spectra, C=O vibrations have a medium intensity and appear at 1792 cm^{-1}. In the fingerprint region, the valence vibrations of C-C bonds of carbon skeleton are clearly visible. These peaks are characterized by medium and low intensity in the range of 600-1200 cm^{-1}, while deformation vibrations of CH_2 bonds are observed at 1300-1500 cm^{-1}.

3.2. Study of the mechanisms of the investigated reactions based on data obtained by in-situ/operando multispectroscopy. Generalization of the obtained results

The reaction was monitored in-situ/operando by two complementary methods, namely IR and Raman spectra. For monitoring, the probes were immersed directly into the reaction mixture, with an initial pressure of 650 kPa (decreasing as the reaction proceeded), constant temperature at 90°C, and catalyst concentration of 2 mol%. Subsequently, scans were taken at fixed time intervals, which were shorter (5-10 minutes) at the start of the reaction.

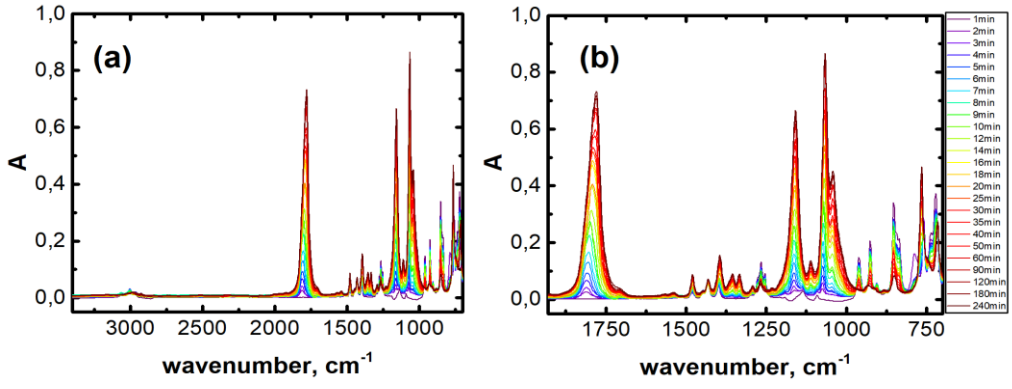

a) b)

Figure 3 IR spectra of the reaction mixture in carboxylation reaction of epichlorohydrin, reaction conditions: p = 650 kPa, temperature 90°C, catalyst 2 mol%: a – region 3400-700 cm^{-1}; b – region 2000-700 cm^{-1}

As the reaction decreases due to the consumption of reactants, there is an increase in the conversion rate (30-60 minutes). IR spectra over the entire wave number range and in the 2000-700 cm^{-1} are shown in Figure 3. Raman spectra of the reaction mixture in the whole range of wave numbers and the range 1-1100 cm^{-1} are presented in Figure 4. In both spectra, the peak of carbonyl group is clearly visible, showing the formation of cyclocarbonate - chloropropylene carbonate. Regarding IR spectra, there are asymmetric vibrations of C=O bonds, with peaks at 1800 cm^{-1}. In the case of Raman spectra, there are symmetric vibrations of the same bond, with medium intensity at 1750 cm^{-1}.

As shown in Figure 4, a strong luminescence is observed, which increases as the concentration of initial epichlorohydrin decreases (weak luminescence). Moreover, peaks are observed in region of equal concentrations of the initial substance and the reaction product, namely 50% conversion. The results suggest that the quenching of luminescence occurs at limiting concentrations of the starting substance (epichlorohydrin) or reaction product (chloropropylene carbonate). The intermediate concentrations are insufficient for the concentration quenching of luminescence to occur. Due to the high luminescence, it is not possible to carry out a sufficient accumulation of substances for scanning. Therefore, in the region of intermediate conversion, the target signals are lost behind luminescence peaks and the informative value of spectra is low. This indicates that Raman spectra prove to be less suitable compared to IR spectra for in-situ operando monitoring tasks.

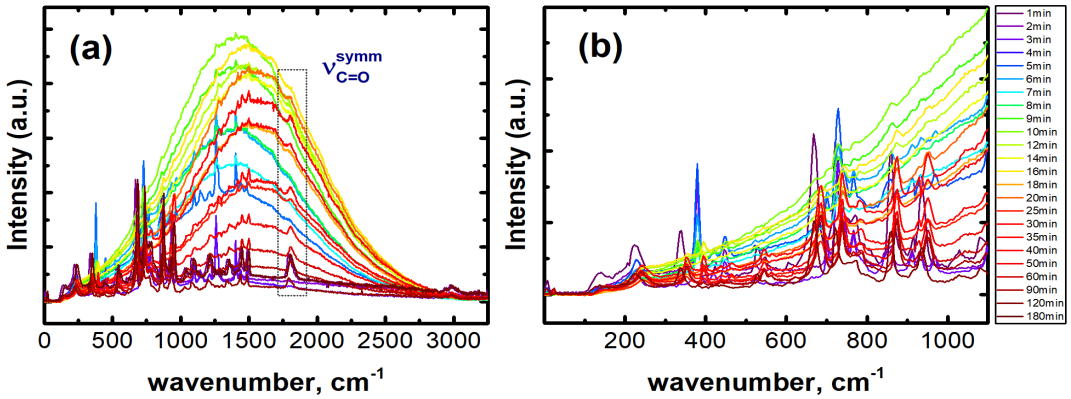

a) b)

Figure 4 Raman spectra of the reaction mixture in carboxylation reaction of epichlorohydrin; reaction conditions: p = 650 kPa, temperature 90°C, catalyst 2 mol%. a - whole range of wave numbers, b - range 1-1100 cm^{-1}

IR spectra provide sufficient information for obtaining detailed information on the reaction process. Specifically, Figure 5 (a) shows spectra of the reaction mixture in the range 1900-1700 cm^{-1}, where the growth of C=O bonds of carbonate fragment is clearly visible. The peak becomes visible 5 minutes after the start of the reaction, indicating the formation of chloropropylene carbonate. Subsequently, the peak apex shifts slightly as the reaction product due to the influence of the solvent, namely initial epichlorohydrin. As a polar solvent, epichlorohydrin affects vibrational frequency of C=O bond of the dissolved chloropropylene carbonate.

As chloropropylene carbonate increases, the concentration of epichlorohydrin decreases. Furthermore, the effect on the absorption band becomes increasingly weaker, reaching zero at the end point of the reaction (conversion of epichlorohydrin is more than 99%). This allows for observation of C=O bonds wave number of carbonate fragment, which is 1778 cm^{-1}. The bands in the 1500–1200 cm^{-1} region, primarily corresponding to C–H deformation, are shown in Figure 5(b). As the product accumulates, new bands corresponding to the vibrations begin to appear with the presence of C-H bonds. The observation is due to the more tense geometry of the three-membered cycle in parent compound, which limits vibrational modes and intensities. In comparison, the more

relaxed structure of the product allows for stronger and defined C–H vibrational bands, which are more intense than reactants.

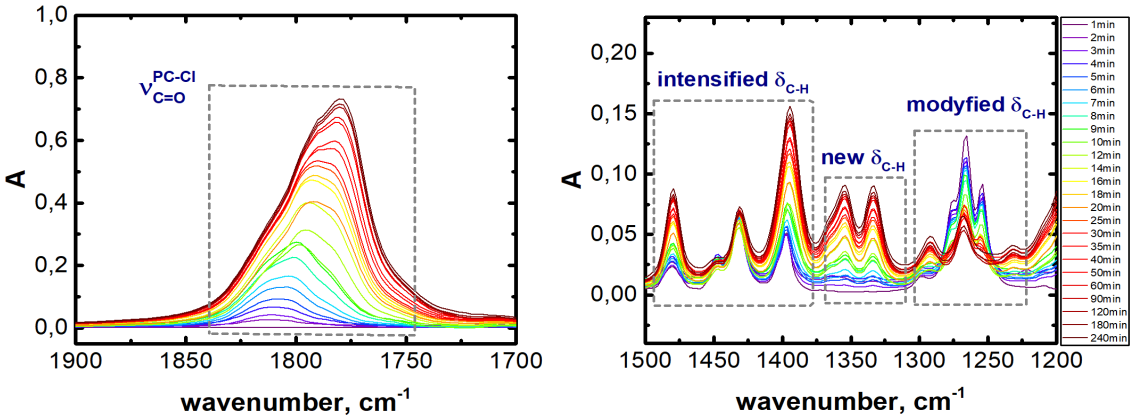

a) b)

Figure 5 IR spectra of the reaction mixture in carboxylation reaction of epichlorohydrin; reaction conditions: p = 1300 kPa, temperature 90°C, catalyst 2 mol%: a – region 1900-1700 cm^{-1}; b – region 1500-1200 cm^{-1}

The absorption bands of C-O-C vibrations of carbonate fragment grow similarly to C=O bonds. Since there are several bonds in the formed carbonate and non-equivalent, numerous increasing bands can be observed in IR spectra (Figure 6(a)). C-O-C bands of the C-O-C bonds of chloropropylene carbonate are at 1158, 1061, and 1037 cm^{-1}. C-O-C bands of the original epichlorohydrin are also visible, showing small peaks at 1137 and 1089 cm^{-1}. These peaks have lower intensity than in chloropropylene carbonate due to the tenseness of the ring (three-membered cycle of epichlorohydrin), bond vibrations, and smaller amplitudes.

The 1000-700 cm^{-1} region of IR spectra is shown in Figure 6 (b). There are mainly skeletal valence and deformation vibrations of C-C bonds, as well as carbon-halogen vibrations (C-Cl). Based on observation, spectra show that vibrations related to the initial epichlorohydrin are decreasing, while those related to the product are increasing. The appearance of new vibrations does not indicate new C-C bonds. However, new modes of vibrations are available in the more labile five-membered chloropropylene carbonate cycle.

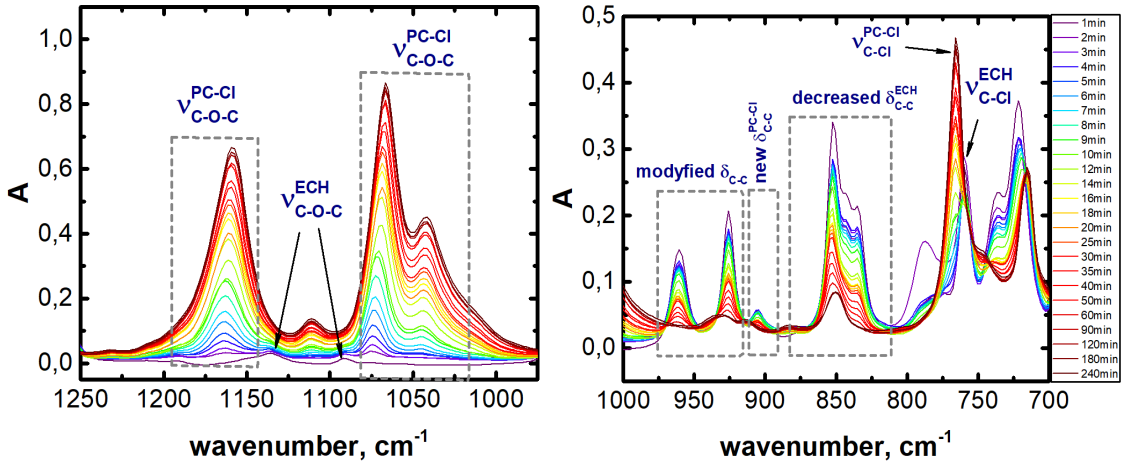

a) b)

Figure 6 IR spectra of the reaction mixture in carboxylation reaction of epichlorohydrin; reaction conditions: p = 1300 kPa, temperature 90°C, catalyst 2 mol%: a – region 1250-950 cm^{-1}; b – region 1000-700 cm^{-1}

Due to the low concentrations, neither IR nor Raman spectra were able to record bands related to the by-products or catalyst. To register these interactions, additional experiments were performed with molar ratio of catalyst to substrate of 1:1. Furthermore, hydroxyl group of the substituent and epoxide (chloropropylene oxide) were evaluated using IR spectra (Figure 7). The analysis was performed to evaluate and determine the presence of hydrogen bonding comprising acidic proton of imidazole. Based on the results, IR spectra of pure 1-(2-hydroxyethyl)-3-methylimidazolium bromide (Figure 7, black) showed a band at 3238 cm^{-1} belonging to the O-H bond vibrations of the hydroxyl group. A band at 3052 cm^{-1} was also observed belonging to C-H proton vibrations at C^2-position of the imidazole ring. After interaction with epichlorohydrin, both bands were simultaneously broadened and shifted to 3279 and 3075 cm^{-1}, respectively (Figure 7, red). The observed frequency shifts of the imidazolium ring could be attributed to the intermolecular interaction between the acidic imidazolium proton, the hydroxyl proton present in IL, and epoxide due to the hydrogen bond. Additionally, out-of-plane strain bands in the fingerprint region were shifted depending on the presence of interaction with epoxide. The strongest interaction and large peak shift were observed between the acidic protons of the imidazolium ring and the oxygen atom of epoxide.

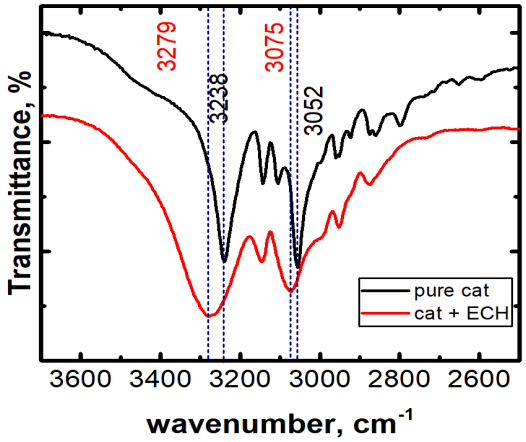

Figure 7 Determination of interactions between catalyst and substrate epoxide by FTIR spectroscopy

Coordination of the acid proton with oxygen atom of epoxide leads to polarisation of C-O bond, which facilitates the opening of epoxide ring (Chatelet et al., 2013; Izgorodina et al., 2009; Dong et al., 2006). At the same time, nucleophilic attack of IL anion (bromide) by the less hindered β-carbon atom of epoxide occurs, alongside cycle opening. This stage is rate-determining for the reaction and the mechanism is discussed based on spectra data.

A schematic of the proposed mechanism is shown in Figure 8. Initially, coordination of epoxide onto catalyst occurs. The process is facilitated by the formation of a hydrogen bond between the oxygen of chloropropylene carbonate and hydrogen of catalyst. This comprises the acidic proton of the imidazolium ring and hydrogen of hydroxyl group of the 2-ethoxy (Chatelet et al., 2013; Dong et al., 2006) substituent of the imidazolium ring. Coordination occurs by both pathways as shown in spectra data, according to the concept that IL with a hydroxyl group in the composition has higher catalytic activity (Jia et al., 2020; Jayakumar et al., 2017). This coordination of the acid proton with oxygen atom of epoxide leads to the polarisation of C-O bond, which facilitates the opening of epoxide ring. Similarly, there is occurrence of the nucleophilic attack of Br-halide anion by the less hindered β carbon atom of epoxide (stage I).

In the next stage, epoxide opens and a proton transfer from hydroxyl group of IL to oxygen takes place. This leads to the formation of an intermediate transient 7-membered cycle including ionic fragments and oxygen of the substrate (stage II). Subsequently, CO_2 molecule coordinates with the system, where oxide oxygen attracts CO_2 carbon with electron density deficiency, causing a reverse

proton transfer to the hydroxyl group (stage III). C-O bond is also formed between carbon of CO_2 and oxygen of chloropropienoxide. The oxygen coordinated to the protons of IL has excessive electron density and attacks the electron-depleted carbon of chloropropylene oxide bound to the easily escaping bromine atom (stage IV). Then, carbonate cycle closes, leading to product formation and regeneration of IL (stage V).

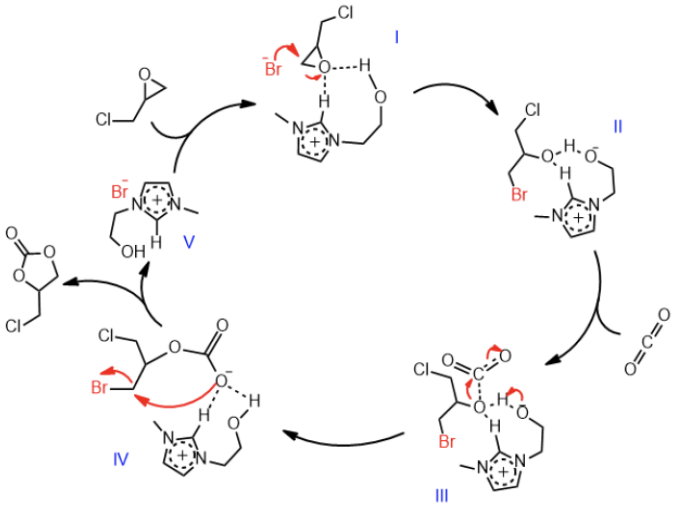

Figure 8 Assumed mechanism of carboxylation reaction

4. Conclusions

In conclusion, this study conducted experimental and analytical complex for in-situ/operando studies. The analysis was based on multispectroscopy using immersion IR and Raman probes operating at high pressure and temperature for spectral screening and analyzing epichlorohydrin carboxylation reaction. Changes in the concentration of initial components (CO_2 and epichlorohydrin) during the experiment were monitored using mass spectra included in the complex. The study allowed recording the enhancement of vibrations corresponding to chloropropylene carbonate as the reaction product accumulated. IR spectra also showed the coordination of the substrate on catalyst, which occurred because of hydrogen bonds between the imidazole proton in C^2 position of the imidazole ring and hydroxyl group of the substituent in IL. This study confirmed the proposed mechanism of catalytic reaction of converting CO_2 into cyclic carbonate. The results showed that IL with a hydroxyl group in the composition had high catalytic activity. In the future, recommendation was made to explore the possibility of using IL as a component for selective extraction of CO_2 from gas mixtures with subsequent conversion into valuable products.

Acknowledgements

This study was funded by the Russian Science Foundation according to research project No. 22-79-10302.

Author Contributions

Maria Atlaskina: Conceptualization, Project administration, Writing – review and editing; Zakhar Markin: Formal analysis, Investigation; Writing – original draft; Kirill Smorodin: Investigation, Methodology; Sergey Kryuchkov: Investigation, Methodology; Pavel Tiuleanu: Software; Alexander Sysoev: Software; Anton Petukhov: Data curation, Validation; Artem Atlaskin: Software, Validation; Olga Kazarina: Data curation, Validation; Andrey Vorotyntsev: Data curation; Ilya Vorotyntsev: Supervision.

Conflict of Interest

Disclose any conflicts of interest, or explicitly state "The authors declare no conflicts of interest.

References

Anggerta, LA, Kurniawansyah, F, Tetrisyanda, R & Wibawa, G 2025, 'Catalytic synthesis of diethyl carbonate from carbon dioxide using catalyst KI/EtONa with propylene oxide as dehydration agent and process optimization based on Box-Behnken design', *International Journal of Technology*, vol. 16, no. 1, pp. 243–254, https://doi.org/10.14716/IJTECH.V16I1.6417

Arstad, B, Fjellvåg, H, Kongshaug, KO, Swang, O & Blom, R 2008, 'Amine functionalised metal organic frameworks (MOFs) as adsorbents for carbon dioxide', *Adsorption*, vol. 14, pp. 755–762, https://doi.org/10.1007/s10450-008-9137-6

Asgharnejad, L, Abbasi, A & Shakeri, A 2018, 'Ni-based metal-organic framework/GO nanocomposites as selective adsorbent for CO_2 over N_2', *Microporous and Mesoporous Materials*, vol. 262, pp. 227–234, https://doi.org/10.1016/J.MICROMESO.2017.11.038

Atlaskina, M, Markin, Z, Smorodin, K, Kryuchkov, S, Tsivkovsky, N, Petukhov, A, Atlaskin, A, Kazarina, O, Vorotyntsev, A & Vorotyntsev, I 2025, 'Optimized CO_2 cycloaddition to epichlorohydrin catalyzed by ionic liquid with microwave and ultrasonic irradiation', *International Journal of Technology*, vol. 16, no. 2, pp. 1-16, https://doi.org/10.14716/ijtech.v16i2.7500

Ayuso, M, Mateo, S, Belinchón, A, Navarro, P, Palomar, J, García, J & Rodríguez, F 2023, 'Cyclic carbonates as solvents in the dearomatization of refinery streams: Experimental liquid–liquid equilibria, modelling, and simulation', *Journal of Molecular Liquids*, vol. 380, article 121710, https://doi.org/10.1016/J.MOLLIQ.2023.121710

Chaker, Y, Ilikti, H, Debdab, M, Moumene, T, Belarbi, EH, Wadouachi, A, Abbas, O, Khelifa, B & Bresson, S 2016, 'Synthesis and characterization of 1-(hydroxyethyl)-3-methylimidazolium sulfate and chloride ionic liquids', *Journal of Molecular Structure*, vol. 1113, pp. 182–190, https://doi.org/10.1016/J.MOLSTRUC.2016.02.017

Chatelet, B, Joucla, L, Dutasta, JP, Martinez, A, Szeto, KC & Dufaud, V 2013, 'Azaphosphatranes as structurally tunable organocatalysts for carbonate synthesis from CO2 and epoxides', *Journal of the American Chemical Society*, vol. 135, pp. 5348–5351, https://doi.org/10.1021/ja402053d

Cruz, OF, Gómez, IC, Rodríguez-Reinoso, F, Silvestre-Albero, J, Rambo, CR & Martínez-Escandell, M 2023, 'Activated carbons with high micropore volume obtained from polyurethane foams for enhanced CO2 adsorption', *Chemical Engineering Science*, vol. 273, article 118671, https://doi.org/10.1016/J.CES.2023.118671

Dinh, CT, Burdyny, T, Kibria, G, Seifitokaldani, A, Gabardo, CM, Pelayo García De Arquer, F, Kiani, A, Edwards, JP, De Luna, P, Bushuyev, OS, Zou, C, Quintero-Bermudez, R, Pang, Y, Sinton, D & Sargent, EH 2018, 'CO2 electroreduction to ethylene via hydroxide-mediated copper catalysis at an abrupt interface', *Science*, vol. 360, pp. 783–787, https://doi.org/10.1126/SCIENCE.AAS9100/SUPPL_FILE/AAS9100-DINH-SM.PDF

Dong, K, Zhang, S, Wang, D & Yao, X 2006, 'Hydrogen bonds in imidazolium ionic liquids', *Anaesthesist*, vol. 110, pp. 9775–9782

Hu, YL, Lu, M & Yang, XL 2015, 'Highly efficient synthesis of cyclic carbonates from carbon dioxide and epoxides catalyzed by ionic liquid [Heemim][ZrCl5]', *RSC Advances*, vol. 5, pp. 67886–67891, https://doi.org/10.1039/c5ra11786k

Izgorodina, EI, Bernard, UL & MacFarlane, DR 2009, 'Ion-pair binding energies of ionic liquids: can DFT compete with ab initio-based methods?', *Journal of Physical Chemistry A*, vol. 113, pp. 7064–7072, https://doi.org/10.1021/jp8107649

Jayakumar, S, Li, H, Zhao, Y, Chen, J & Yang, Q 2017, 'Cocatalyst-free hybrid ionic liquid (IL)-based porous materials for efficient synthesis of cyclic carbonates through a cooperative activation pathway', *Chemistry – An Asian Journal*, vol. 12, pp. 577–585, https://doi.org/10.1002/asia.201601676

Jessop, PG 2011, 'Searching for green solvents', *Green Chemistry*, vol. 13, pp. 1391–1398, https://doi.org/10.1039/C0GC00797H

Jia, D, Ma, L, Wang, Y, Zhang, W, Li, J, Zhou, Y & Wang, J 2020, 'Efficient CO2 enrichment and fixation by engineering micropores of multifunctional hypercrosslinked ionic polymers', *Chemical Engineering Journal*, vol. 390, article 124652, https://doi.org/10.1016/j.cej.2020.124652

Jin, F, Wang, R, Liu, Y, Zhang, N, Bao, C, Li, D, Wang, D, Cheng, T, Liu, H, Dou, S & Wang, B 2024, 'Conversion mechanism of sulfur in room-temperature sodium-sulfur battery with carbonate-based electrolyte', *Energy Storage Materials*, vol. 69, article 103388, https://doi.org/10.1016/j.ensm.2024.103388

Jou, FY, Mather, AE & Otto, FD 1995, 'The solubility of CO2 in a 30 mass percent monoethanolamine solution', *Canadian Journal of Chemical Engineering*, vol. 73, pp. 140–147, https://doi.org/10.1002/cjce.5450730116

Kadiwala, S, Rayer, AV & Henni, A 2010, 'High pressure solubility of carbon dioxide (CO2) in aqueous piperazine solutions', *Fluid Phase Equilibria*, vol. 292, pp. 20–28, https://doi.org/10.1016/j.fluid.2010.01.009

Kamphuis, AJ, Picchioni, F & Pescarmona, PP 2019, 'CO2-fixation into cyclic and polymeric carbonates: principles and applications', *Green Chemistry*, vol. 21, pp. 406–448, https://doi.org/10.1039/C8GC03086C

Kartohardjono, S, Paramitha, A, Putri, AA & Andriant, R 2017, 'Effects of absorbent flow rate on CO2 absorption through a super hydrophobic hollow fiber membrane contactor', *International Journal of Technology*, vol. 8, pp. 1429–1435, https://doi.org/10.14716/IJTECH.V8I8.679

Kazarina, OV, Agieienko, VN, Petukhov, AN, Vorotyntsev, AV, Kazarin, AS, Atlaskina, ME, Atlaskin, AA, Markov, AN, Golovacheva, AA & Vorotyntsev, IV 2022, 'Monoethanolamine + Ethylene Glycol + Choline Chloride: An effect of the mixture composition on the CO_2 absorption capacity, density, and viscosity', *Journal of Chemical and Engineering Data*, vol. 67, pp. 2899–2912, https://doi.org/10.1021/acs.jced.2c00245

Kryuchkov, S, Smorodin, K, Stepakova, A, Atlaskin, A, Tsivkovsky, N, Atlaskina, M, Tolmacheva, M, Kazarina, O, Petukhov, A, Vorotyntsev, A & Vorotyntsev, I 2024, 'Membrane air separation process simulation: Insight in modelling approach based on ideal and mixed permeance values', *International Journal of Technology*, vol. 15, pp. 1218–1236, https://doi.org/10.14716/IJTECH.V15I5.6987

Kumar, B, Brian, JP, Atla, V, Kumari, S, Bertram, KA, White, RT & Spurgeon, JM 2016, 'New trends in the development of heterogeneous catalysts for electrochemical CO2 reduction', *Catalysis Today*, vol. 270, pp. 19–30, https://doi.org/10.1016/j.cattod.2016.02.006

Kusrini, E, Utami, CS, Usman, A, Nasruddin & Tito, KA 2018, 'CO2 capture using graphite waste composites and ceria', *International Journal of Technology*, vol. 9, no. 2, pp. 287–296, https://doi.org/10.14716/IJTECH.V9I2.1031

Le Quéré, C, Andrew, RM, Canadell, JG, Sitch, S, Korsbakken, JI, Peters, GP, Manning, AC, Boden, TA, Tans, PP, Houghton, RA, Keeling, RF, Alin, S, Andrews, OD, Anthoni, P, Barbero, L, Bopp, L, Chevallier, F, Chini, LP, Ciais, P, Currie, K, Delire, C, Doney, SC, Friedlingstein, P, Gkritzalis, T, Harris, I, Hauck, J, Haverd, V, Hoppema, M, Goldewijk, KG, Jain, AK, Kato, E, Körtzinger, A, Landschützer, P, Lefèvre, N, Lenton, A, Lienert, S, Lombardozzi, D, Melton, JR, Metzl, N, Millero, F, Monteiro, PMS, Munro, DR, Nabel, JEMS, Nakaoka, SI, O'Brien, K, Olsen, A, Omar, AM, Ono, T, Pierrot, D, Poulter, B, Rödenbeck, C, Salisbury, J, Schuster, U, Schwinger, J, Séférian, R, Skjelvan, I, Stocker, BD, Sutton, AJ, Takahashi, T, Tian, H, Tilbrook, B, Van Der Laan-Luijkx, IT, Van Der Werf, GR, Viovy, N, Walker, AP, Wiltshire, AJ & Zaehle, S 2016, 'Global carbon budget 2016', *Earth System Science Data*, vol. 8, no. 2, pp. 605–649, https://doi.org/10.5194/essd-8-605-2016

Li, F, Thevenon, A, Rosas-Hernández, A, Wang, Z, Li, Y, Gabardo, CM, Ozden, A, Dinh, CT, Li, J, Wang, Y, Edwards, JP, Xu, Y, McCallum, C, Tao, L, Liang, ZQ, Luo, M, Wang, X, Li, H, O'Brien, CP, Tan, CS, Nam, DH, Quintero-Bermudez, R, Zhuang, TT, Li, YC, Han, Z, Britt, RD, Sinton, D, Agapie, T, Peters, JC & Sargent, EH 2019, 'Molecular tuning of CO_2-to-ethylene conversion', *Nature*, vol. 577, pp. 509–513, https://doi.org/10.1038/s41586-019-1782-2

Liu, M, Gao, K, Liang, L, Wang, F, Shi, L, Sheng, L & Sun, J 2015, 'Insights into hydrogen bond donor promoted fixation of carbon dioxide with epoxides catalyzed by ionic liquids', *Physical Chemistry Chemical Physics*, vol. 17, pp. 5959–5965, https://doi.org/10.1039/c4cp05464d

Liu, S, Xiao, J, Lu, XF, Wang, J, Wang, X & Lou, XW 2019, 'Efficient electrochemical reduction of CO_2 to HCOOH over sub-2 nm SnO_2 quantum wires with exposed grain boundaries', *Angewandte Chemie International Edition*, vol. 58, pp. 8499–8503, https://doi.org/10.1002/anie.201903613

Lu, X, Leung, DYC, Wang, H, Leung, MKH & Xuan, J 2014, 'Electrochemical reduction of carbon dioxide to formic acid', *ChemElectroChem*, vol. 1, pp. 836–849, https://doi.org/10.1002/celc.201300206

Madani, H, Wibowo, A, Sasongko, D, Miyamoto, M, Uemiya, S & Budhi, YW 2024, 'Novel multiphase CO_2 photocatalysis system using N-TiO_2/CNCs and CO_2 nanobubble', *International Journal of Technology*, vol. 15, no. 2, pp. 432–441, https://doi.org/10.14716/ijtech.v15i2.6694

Maina, JW, Pozo-Gonzalo, C, Kong, L, Schütz, J, Hill, M & Dumée, LF 2017, 'Metal organic framework based catalysts for CO_2 conversion', *Materials Horizons*, vol. 4, no. 3, pp. 345–361, https://doi.org/10.1039/c6mh00484a

Mohammadi, A & Nakhaei Pour, A 2023, 'Triethylenetetramine-impregnated ZIF-8 nanoparticles for CO_2 adsorption', *Journal of CO_2 Utilization*, vol. 69, article 102424, https://doi.org/10.1016/j.jcou.2023.102424

NIST U.S. Department of Commerce 2014, NIST Standard Reference Database 69, NIST Chemistry WebBook, SRD 69, viewed 10 January 2025, (https://webbook.nist.gov/cgi/cbook.cgi?ID=C106898&Units=SI&Mask=200#Mass-Spec)

North, M 2012, 'Synthesis of cyclic carbonates from epoxides and carbon dioxide using bimetallic aluminium(salen) complexes', *Arkivoc*, vol. 2012, pp. 610–628, https://doi.org/10.3998/ark.5550190.0013.115

Olaniyan, B & Saha, B 2020, 'Comparison of catalytic activity of ZIF-8 and Zr/ZIF-8 for greener synthesis of chloromethyl ethylene carbonate by CO_2 utilization', *Energies*, vol. 13, no. 3, https://doi.org/10.3390/en13030521

Ozden, A, Wang, Y, Li, F, Luo, M, Sisler, J, Thevenon, A, Rosas-Hernández, A, Burdyny, T, Lum, Y, Yadegari, H, Agapie, T, Peters, JC, Sargent, EH & Sinton, D 2021, 'Cascade CO_2 electroreduction enables efficient carbonate-free production of ethylene', *Joule*, vol. 5, no. 3, pp. 706–719, https://doi.org/10.1016/j.joule.2021.01.007

Qian, Y, Chu, Y, Zheng, Z, Shadike, Z, Han, B, Xiang, S, Kang, Y, Hu, S, Cao, C, Zhong, L, Shi, Q, Lin, M, Zeng, H, Wang, J, Hu, E, Weiland, C, Yang, XQ & Deng, Y 2022, 'A new cyclic carbonate enables high power/low temperature lithium-ion batteries', *Energy Storage Materials*, vol. 45, pp. 14–23, https://doi.org/10.1016/j.ensm.2021.11.029

Schreiber, MW 2024, 'Industrial CO_2 electroreduction to ethylene: Main technical challenges', *Current Opinion in Electrochemistry*, vol. 44, article 101438, https://doi.org/10.1016/j.coelec.2023.101438

Shah, HUR, Ahmad, K, Bashir, MS, Shah, SSA, Najam, T & Ashfaq, M 2022, 'Metal organic frameworks for efficient catalytic conversion of CO_2 and CO into applied products', *Molecular Catalysis*, vol. 517, article 112055, https://doi.org/10.1016/j.mcat.2021.112055

Shariff, AM, Shaikh, MS, Bustam, MA, Garg, S, Faiqa, N & Aftab, A 2016, 'High-pressure solubility of carbon dioxide in aqueous sodium L-prolinate solution', *Procedia Engineering*, vol. 148, pp. 580–587, https://doi.org/10.1016/j.proeng.2016.06.516

Souza-Filho, JDV, Oliveira, ES, Guedes, JB, Silva Júnior, JBA, Alves, CRF, Coelho, JA, Lima, ACA, Bastos-Neto, M, Sasaki, JM, Mota, FSB & Loiola, AR 2024, 'Zeolite A grown on fiberglass: A prominent CO_2 adsorbent for CO_2/CH_4 separation', *Colloids and Surfaces A: Physicochemical and Engineering Aspects*, vol. 683, article 132952, https://doi.org/10.1016/j.colsurfa.2023.132952

Sridhar, N, Zhai, Y, Agarwal, A & Chiacchiarelli, L 2009, 'Effect of gaseous impurities on the electrochemical reduction of CO_2 on copper electrodes', *ECS Meeting Abstracts*, vol. MA2009-01, article 1473, https://doi.org/10.1149/ma2009-01/44/1473

Su, W, Zhong, S & Fan, Y 2024, 'A novel Cu-based covalent organic framework with Cu-N2O2 single sites for efficient CO_2 electroreduction to methane', *Applied Catalysis B: Environmental*, vol. 354, article 124145, https://doi.org/10.1016/j.apcatb.2024.124145

Sun, J, Zhang, S, Cheng, W & Ren, J 2008, 'Hydroxyl-functionalized ionic liquid: A novel efficient catalyst for chemical fixation of CO_2 to cyclic carbonate', *Tetrahedron Letters*, vol. 49, no. 21, pp. 3588–3591, https://doi.org/10.1016/j.tetlet.2008.04.022

Tillmann, SD, Isken, P & Lex-Balducci, A 2014, 'Gel polymer electrolyte for lithium-ion batteries comprising cyclic carbonate moieties', *Journal of Power Sources*, vol. 271, pp. 239–244, https://doi.org/10.1016/j.jpowsour.2014.07.185

Wang, JQ, Cheng, WG, Sun, J, Shi, TY, Zhang, XP & Zhang, SJ 2014, 'Efficient fixation of CO_2 into organic carbonates catalyzed by 2-hydroxymethyl-functionalized ionic liquids', *RSC Advances*, vol. 4, no. 6, pp. 2360–2367, https://doi.org/10.1039/c3ra45918g

Whang, HS, Lim, J, Choi, MS, Lee, J & Lee, H 2019, 'Heterogeneous catalysts for catalytic CO_2 conversion into value-added chemicals', *BMC Chemical Engineering*, vol. 1, no. 1, pp. 1–19, https://doi.org/10.1186/s42480-019-0007-7

Whiteoak, CJ, Kielland, N, Laserna, V, Castro-Gõmez, F, Martin, E, Escudero-Adán, EC, Bo, C & Kleij, AW 2014, 'Highly active aluminium catalysts for the formation of organic carbonates from CO_2 and oxiranes', *Chemistry – A European Journal*, vol. 20, no. 8, pp. 2264–2275, https://doi.org/10.1002/chem.201302536

Yaashikaa, PR, Senthil Kumar, P, Varjani, SJ & Saravanan, A 2019, 'A review on photochemical, biochemical and electrochemical transformation of CO_2 into value-added products', *Journal of CO_2 Utilization*, vol. 33, pp. 131–147, https://doi.org/10.1016/j.jcou.2019.05.017

Yan, T, Liu, H, Zeng, ZX & Pan, WG 2023, 'Recent progress of catalysts for synthesis of cyclic carbonates from CO_2 and epoxides', *Journal of CO_2 Utilization*, vol. 68, article 102355, https://doi.org/10.1016/j.jcou.2022.102355

Yuan, J, Wang, Y, Tang, M, Hao, X, Liu, J, Zhang, G & Zhang, Y 2023, 'Preparation of N, O co-doped carbon nanotubes and activated carbon composites with hierarchical porous structure for CO_2 adsorption by coal pyrolysis', *Fuel*, vol. 333, no. 2, article 126465, https://doi.org/10.1016/j.fuel.2022.126465

Yulia, F, Utami, VJ, Nasruddin & Zulys, A 2019, 'Synthesis, characterizations, and adsorption isotherms of CO_2 on chromium terephthalate (MIL-101) metal-organic frameworks (MOFs)', *International Journal of Technology*, vol. 10, no. 7, pp. 1427–1436, https://doi.org/10.14716/IJTECH.V10I7.3706

Zaoui, T, Debdab, M, Haddad, B, Belarbi, EH, Chaker, Y, Rahmouni, M, Bresson, S & Baeten, V 2021, 'Synthesis, vibrational and thermal properties of new functionalized 1-(2-hydroxyethyl)-3-methylimidazolium dihydrogenophosphate ionic liquid', *Journal of Molecular Structure*, vol. 1236, article 130264, https://doi.org/10.1016/j.molstruc.2021.130264

Zha, J, Ding, T, Chen, J, Wang, R, Gao, G & Xia, F 2020, 'Reaction mechanism of CO_2 and styrene oxide catalyzed by ionic liquids: A combined DFT calculation and experimental study', *Journal of Physical Chemistry A*, vol. 124, no. 39, pp. 7991–7998, https://doi.org/10.1021/acs.jpca.0c04662

Zhang, B, Zhang, J, An, P, Su, Z, Wan, Q, Tan, X & Zheng, L 2021, 'Steering CO_2 electroreduction toward methane or ethylene production', *Nano Energy*, vol. 88, article 106239, https://doi.org/10.1016/j.nanoen.2021.106239

Zhang, G & Xu, Z 2024, 'CO_2 Conversion via MOF-based catalysts', *Advances in CO_2 Utilization*, pp. 1-36, https://doi.org/10.1007/978-981-99-8822-8_1

Zhang, T, Verma, S, Kim, S, Fister, TT, Kenis, PJA & Gewirth, AA 2020, 'Highly dispersed, single-site copper catalysts for the electroreduction of CO_2 to methane', *Journal of Electroanalytical Chemistry*, vol. 875, article 113862, https://doi.org/10.1016/j.jelechem.2020.113862